Detection and sizing of extended partial blockages in pipelines by means of a stochastic successive linear estimator

Christian Massari, Tian Chyi J. Yeh, Marco Ferrante, Bruno Brunone and Silvia Meniconi

ABSTRACT

Effective water system management depends upon knowledge of the current state of a water pipeline system network. For example, in many cases, partial blockages in a water pipeline system are a source of inefficiencies, and result in an increase of pumping costs. These anomalies must be detected and corrected as early as possible. In this study, an algorithm is developed for detecting blockages by means of pressure transient measurements and estimating the diameter distribution resulting from their formation. The algorithm is a stochastic successive linear estimator that provides statistically the best unbiased estimate of diameter distribution due to partial blockages and quantifies the uncertainty associated with these estimates. We first present the theoretical formulation of the algorithm and then test it with a numerical case study.

Key words | inverse problem, partial extended blockages, pipe systems, primary information, stochastic linear estimator, transient tests

Christian Massari
Marco Ferrante (corresponding author)
Bruno Brunone
Silvia Meniconi
Dipartimento di Ingegneria Civile Ambientale,
Università degli Studi di Perugia,
Via Duranti 93,
Perugia, 06125,
Italy
E-mail: *ferrante@unipg.it*

Tian Chyi J. Yeh
Department of Hydrology and Water Resources,
University of Arizona,
1133 E James E. Rogers Way,
Tucson, AZ 8572,
USA

INTRODUCTION

Partial blockages in pipelines – due to, for example, deposition of sediments, fouling processes and corrosion – cause a reduction of pipe area. A first distinction of partial blockages is based on their length. The literature distinguishes between discrete blockages – where the part of the pipe with a reduced area is much smaller than its total length – and extended blockages, which may occur along a large part of the pipeline. Partial blockages in water pipe networks may contribute to large energy dissipation throughout the system and reduce the service effectiveness for the customers. As a result, they have to be detected and removed as soon as possible.

Conventional methods for locating and sizing partial blockages are based on direct measurements made throughout the pipe system by inspection or intrusive procedures (Gooch *et al.* 1996; Scott & Satterwhite 1998; Scott & Yi 1999). In addition, new techniques based on the use of pipe scanning by radio-isotope technology

(www.tracerco.com) or gamma ray emission (Sharma *et al.* 2010) are available. These methods provide useful information about the state of the pipe, but they are highly time-consuming and costly techniques. Low-cost and quick techniques are of paramount importance in detecting partial blockages because, in addition to cost reduction, they also help to diminish service interruption times. An impetus for research activity in this field has resulted from the use of transient tests as a tool of diagnosis (e.g. Liggett & Chen 1994; Brunone 1999; Vítkovský *et al.* 2000; Brunone & Ferrante 2001; Ferrante & Brunone 2003a, b; Kapelan *et al.* 2003; Mohapatra *et al.* 2006; Lee *et al.* 2008; Ferrante *et al.* 2009; Meniconi *et al.* 2011a, b, c, d, 2012; Duan *et al.* 2012). In particular, in partial blockage detection, Wang *et al.* (2005) examined the effect of discrete blockages on the transient pressure signal. By expressing the analytical solution in terms of a Fourier series, the authors showed that the magnitude and

position of the partial blockage determine a damping on fluid transients that can be used to estimate its size and location. Mohapatra *et al.* (2006) used a systematic procedure to size and locate the partial blockage using a frequency response method for steady oscillatory flow, while Lee *et al.* (2008) proposed to locate and size discrete blockages by extracting the behavior of the system in the form of a frequency response diagram. In all these papers, the partial blockage was considered as a localized occlusion and was modeled by a partially closed in-line valve.

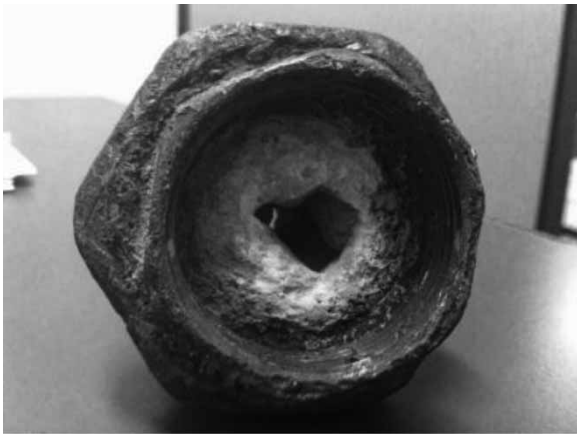Brunone *et al.* (2008a) numerically showed that the length of an extended reduction of the pipe has a

Figure 1 │ Section of steel pipe containing a calcium carbonate partial blockage. Other sections of the same pipe show significantly different geometry.

significantly different impact on the system response in contrast to the presence of an in-line valve. Experiments conducted on smaller diameter trunk mains of different lengths to simulate the extended blockage behavior confirmed these results (Meniconi *et al.* 2011b, 2012). The pressure signal response is different for an in-line valve compared to that of an extended diameter reduction. In Duan *et al.* (2012), the detection of extended blockages was carried out by analyzing the shifting of the resonant peaks of the frequency of the system in transient conditions.

During the formation of a partial blockage, the pipe is characterized by different pipe areas (Figure 1) at different locations due to the complex interaction between the flow and the water chemistry (Hunt 1996).

In these conditions, the area reductions can occur over a large part of the pipe length and may appear as being randomly distributed along the pipe. To properly simulate this feature, in this paper, partial extended blockages are modeled by assigning an equivalent diameter distribution, $D(x)$, able to describe the spatial variations of the area reductions (Massari *et al.* 2012). This approach significantly differs with respect to others in the cited literature, where the problem unknowns are the blockage diameter, D_b, length, L_b, and location, x_b (Figure 2).

The algorithm presented in this paper is based on a geostatistical technique. Geostatistical techniques have been widely used in groundwater hydrology to estimate random fields, i.e. transmissivity, head, velocity, concentration of
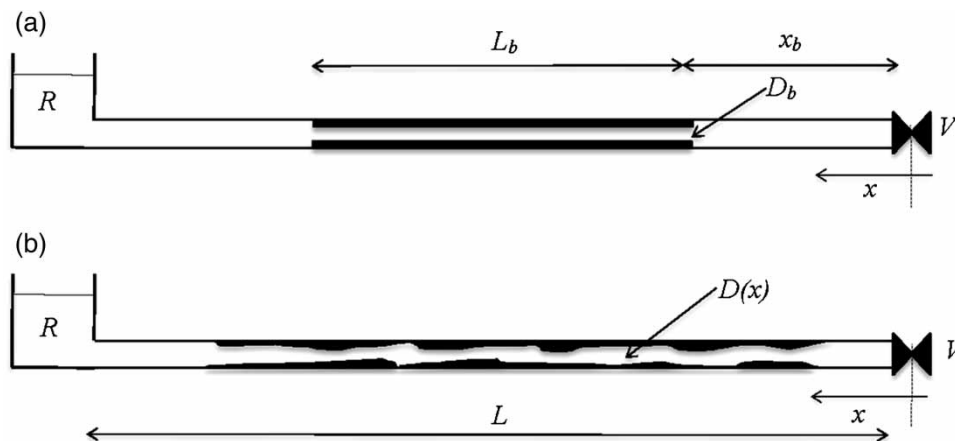

Figure 2 │ Modeling of the extended partial blockage according to (a) Brunone *et al.* (2008a) and Duan *et al.* (2012) and (b) Massari *et al.* (2012). *V* and *R* stand for valve and reservoir, respectively.

pollutants in aquifers and water content in the vadose zone (Kitanidis & Vomvoris 1983; Hoeksema & Kitanidis 1984; Yeh & Zhang 1996; Zhang & Yeh 1997). Such inverse approaches rely on the use of the co-kriging estimation technique, which is based on the assumption of (i) a linear relationship between the involved quantities and (ii) a Gaussian stochastic process (Kitanidis & Vomvoris 1983). However, the assumption of linearity when dealing with non-linear systems is an important limitation of the method (Yeh *et al.* 1996). Such limitations have been overcome by Yeh *et al.* (1996), Zhang & Yeh (1997), Vargas-Guzmán & Yeh (2002), and Zhu & Yeh (2005) by introducing a stochastic successive linear estimator (SLE) approach that considers successive improvements of the estimates by solving the governing flow equations and updating the covariance and cross-covariance matrices of the parameters and hydraulic head fields in an iterative manner. The algorithm has been successfully used in the framework of the hydraulic tomography technique for the estimation of hydrologic parameters of the soil (Yeh & Liu 2000), and tested in many numerical and laboratory case studies (Illman & Liu 2007; Illman *et al.* 2010).

The aim of this paper is to apply the SLE to predict the diameter distribution of partial blockages by casting the inverse problem of the diagnosis in a probabilistic framework. The algorithm takes advantage of diameter measurements along the pipe (primary information) and pressure signals recorded in transient conditions (secondary information) to (i) estimate the diameter distribution resulting from the formation of a partial blockage and (ii) provide the uncertainty associated with these estimates. This feature, i.e. the capability of the parameter uncertainty estimate, is receiving an increasing amount of interest in the analysis of water distribution systems (e.g. Pasha & Lansey 2010; Sun *et al.* 2011; Haghighi & Keramat 2012).

MATHEMATICAL FORMULATION

Governing equations

One-dimensional water hammer flows are governed by the following system of hyperbolic partial differential equations (Wylie & Streeter 1993):

$$\begin{cases} \dfrac{\partial h}{\partial t} + \dfrac{c^2}{gA} \dfrac{\partial Q}{\partial x} = 0 \\ \dfrac{\partial Q}{\partial t} + gA \dfrac{\partial h}{\partial x} + \lambda \dfrac{|Q|Q}{2DA} = 0 \end{cases} \tag{1}$$

where t is the time, x is the location, g is the acceleration due to gravity, h is the head, Q is the discharge, λ is the Darcy–Weisbach friction factor, c is the pressure wave speed, D is the pipe diameter, and A is the pipe area. The system of Equation (1) is subjected to appropriate boundary conditions. At the pipe system locations, x_r, where h is assigned (e.g. reservoirs with known head), it is $h(x_r) = h^*(t)$, while at the valve, it is $\delta(x_v) = \chi Q^2/2gA^2$, where δ is the head minor loss due to the valve, x_v is the valve location and χ is the minor loss coefficient as a function of the valve opening. In order to solve problem (1), appropriate initial conditions (e.g. steady-state conditions) are needed in the domain of analysis.

The head and discharge values are calculated by discretizing and solving the problem by the method of characteristics, leading to the following matrix form (Liggett & Chen 1994):

$$\{u\} = [M]^{-1}\{R\} \tag{2}$$

where $[M]$ is the coefficient matrix,

$$\{u\} = \left\{ \begin{array}{c} h \\ Q \end{array} \right\}$$

is the solution vector of the head and discharge, and $\{R\}$ is the vector associated with the boundary conditions. Equation (2) defines a non-linear system of equations and must be solved at each time step.

Inverse algorithm

In the framework of statistics, an extended partial blockage – modeled as a discrete distribution of diameters along the pipe – can be considered as a stationary stochastic process and the actual distribution of diameters, a single realization among an infinite population of realizations (the ensemble). If the value of the diameter at some locations is known, a variogram analysis can yield a first estimate of the diameter

at unsampled locations. Then, head measurements coming from transient tests at different sections of the pipe system may be used iteratively to improve the first estimate. By means of this procedure, the prediction of the diameter field at unsampled locations is carried out by means of fusing prior information (known diameters at sampled locations) and the secondary one (heads) by means of the SLE. Thus, when prior information is available, it can be embedded in the estimation procedure helping to speed up the inverse algorithm and to improve its accuracy; if not, only head measurements are used.

Let us assume that the pipe diameter, D, is a stationary stochastic process with a constant unconditional mean $Y_d = E[\ln D]$ and unconditional log-perturbation $d(x)$, i.e. $\ln D(x) = Y_d + d(x)$ ($E[\bullet]$ denotes the expected value operator). The corresponding hydraulic head h is given by $h(x) = \Phi(x) + \phi(x)$ where $\Phi(x) = E[h(x)]$ and $\phi(x)$ is the unconditional head perturbation. Since all variables are treated as stochastic processes, an infinite number of possible realizations of $\ln D(x)$ exist in the ensemble. As a result, a solution of the inverse problem is to use the head and pipe diameter values that preserve the observed heads and diameters at sampled locations and satisfy the governing flow equations, as well as the underlying statistical properties associated with the parameters. Such random fields are conditioned realizations of $h(x)$ and $\ln D(x)$ in the ensemble. The goal of the inverse algorithm is to derive the expected value of all these possible conditioned realizations.

By assuming that d and ϕ are jointly normal, their conditional mean estimates at unsampled locations, x_0, can be expressed by a linear combination of the weighted observed values of d and ϕ. That is,

$$\hat{d}(x_0) = \sum_{j=1}^{N_d} \lambda_{dj} d(x_j) + \sum_{k=1}^{N_\phi} \beta_{dk} \phi(x_k) \tag{3}$$

where $\hat{d}(x_0)$ is the co-kriged value at location x_0, N_d is the number of observed diameters and N_ϕ is the number of observed heads. The weights λ_{dj} and β_{dk} are evaluated by requiring that the estimation expressed by Equation (3) will have a minimum variance:

$$E\left[\left(\hat{d} - d\right)^2\right] = \min \tag{4}$$

By substituting Equation (3) into Equation (4), and taking the derivative with respect to λ and β, a linear system of equations is obtained in terms of the covariance matrices, $[C_{dd}]$ and $[C_{\phi\phi}]$, and the cross-covariance matrix, $[C_{\phi d}]$, between ϕ and d:

$$\sum_{pj=1}^{N_d} \lambda_{dj} C_{dd}(x_j, x_{pj}) + \sum_{pk=1}^{N_\phi} \beta_{dk} C_{d\phi}(x_j, x_{pk}) = C_{dd}(x_j, x_0)$$
$$\sum_{pj=1}^{N_d} \lambda_{dj} C_{d\phi}(x_k, x_{pj}) + \sum_{pk=1}^{N_\phi} \beta_{dk} C_{\phi\phi}(x_k, x_{pk}) = C_{\phi d}(x_k, x_0) \tag{5}$$

The covariance $[C_{\phi\phi}]$ and the cross-covariance $[C_{\phi d}]$ in Equation (5) are derived from a first-order numerical approximation (described below) for its flexibility for cases with bounded domain and non-stationary problems.

The values of the diameter are then obtained by:

$$D(x_0) = \exp[d(x_0) + Y_d(x_0)] \tag{6}$$

The uncertainties associated with the estimates are calculated by evaluating the conditional covariance:

$$\varepsilon_{dd} = E\left[\left(d - \hat{d}\right)\left(d - \hat{d}\right)\right] \tag{7}$$

which leads to:

$$\varepsilon_{dd}^{(1)}(x_0, x_0) = C_{dd}(x_0, x_0) - \sum_{j=1}^{N_d} \lambda_{dj} C_{dd}(x_j, x_0)$$
$$- \sum_{k=1}^{N_\phi} \beta_{dk} C_{d\phi}(x_k, x_0) \tag{8}$$

To account for the non-linear relationship between d and h not embedded in the co-kriging, an SLE is used. That is,

$$\hat{Y}_d^{(r+1)}(x_0) = \hat{Y}_d^{(r)}(x_0) + \sum_{j=1}^{N_\phi} \omega_{j0}^d \left[h_j^*(x_j) - h_j^{(r)}(x_j)\right] \tag{9}$$

where ω_{j0}^d are the weighting coefficients for the estimate at x_0 with respect to the head measurements at locations x_j and r is the iteration index. $\hat{Y}_d(x_0)$ is the estimate of the conditional mean of $\ln D(x_0)$, h_j^* is the observed head at

location x_j, while $h_j^{(r)}$ is the simulated head at the same location based on the estimates at the *r*th step. In order for the estimator to have a minimal variance, the optimal weights must be selected according to the mean square error criterion:

$$
\begin{aligned}
E&\left\{\left[\left(\ln D - \hat{Y}_d^{(r)}\right) - \sum_{j=1}^{N_\phi} \omega_{j0}^{d(r)}\left(h_j^* - h_j^{(r)}\right)\right]^2\right\} \\
&= E\left[\left(y_d^{(r)} - \sum_{j=1}^{N_\phi} \omega_{j0}^{d(r)}\phi_j^{(r)}\right)^2\right] \\
&= E\left[\left(y_d^{(r)}\right)^2 - 2\sum_{j=1}^{N_\phi}\omega_{j0}^{d(r)}y_d^{(r)}\phi_j^{(r)} + \sum_{j=1}^{N_\phi}\sum_{k=1}^{N_\phi}\omega_{j0}^{d(r)}\omega_{k0}^{d(r)}\phi_j^{(r)}\phi_k^{(r)}\right] \\
&= \varepsilon_{yy}^{d(r)} - \sum_{k=1}^{N_\phi}\omega_{j0}^{d(r)}\varepsilon_{y\phi}^{d(r)} + \sum_{j=1}^{N_\phi}\sum_{k=1}^{N_\phi}\omega_{j0}^{d(r)}\omega_{k0}^{d(r)}\varepsilon_{\phi\phi}^{d(r)}
\end{aligned}
\tag{10}
$$

where $y_d^{(r)}$ is the residual about the mean estimate, while $\varepsilon_{yy}^{d(r)}$, $\varepsilon_{y\phi}^{d(r)}$ and $\varepsilon_{\phi\phi}^{d(r)}$ are error covariances and cross-covariances at iteration *r*. The weights are determined by taking the derivative of Equation (10) with respect to ω and set the resultant equal to zero. The following system of equations is obtained:

$$
\sum_{j=1}^{N_\phi}\omega_{j0}^{d(r)}\varepsilon_{\phi\phi}^{(r)}(x_j, x_l) + \theta\delta_{jl} = \varepsilon_{y\phi}^{d(r)}(x_0, x_l)
\tag{11}
$$

where $\left[\varepsilon_{\phi\phi}\right]$ and $\left[\varepsilon_{y\phi}\right]$ are the conditional covariance and the conditional cross-covariance matrices, respectively, at each iteration and $[\delta_{jl}]$ is the identity matrix. During each iteration, a term, θ, is added to the diagonal terms of $\left[\varepsilon_{\phi\phi}\right]$ to ensure a stable solution. The value of θ is determined as the product of a constant weighting factor and the maximum value of $\left[\varepsilon_{\phi\phi}\right]$ at each iteration (Yeh & Zhang 1996). The approach is analogous to the pseudo transient technique employed for non-linear numerical problems described by Fletcher (1988).

The matrices $\left[\varepsilon_{\phi\phi}\right]$ and $\left[\varepsilon_{y\phi}\right]$ are approximated at each iteration on the basis of the first-order analysis (Dettinger & Wilson 1981) in which the heads at the *r*th iteration can be written as a first-order Taylor series expansion:

$$
\{h\} = \{\Phi\} + \{\phi\} = \mathbf{G}(\{Y_d\} + \{d\}) \approx \mathbf{G}\{Y_d\} + \left[J^d\right]\{\ln D - Y_d\}
\tag{12}
$$

where $\mathbf{G}$ is the vector function describing Equation (2) and $\left[J^d\right]$ is the sensitivity matrix of the head with respect to the log-diameter:

$$
\left[J^d\right] \approx \frac{\partial \mathbf{G}(\{Y_d\})}{\partial\{\ln D\}}
\tag{13}
$$

Equation (12) can be rewritten as:

$$
\{\phi\} \approx [J_d]\{d\}
\tag{14}
$$

and it is used to calculate the approximate covariance of the heads and the cross-covariance between the heads and the diameters:

$$
\begin{aligned}
\left[\varepsilon_{\phi\phi}^{(r)}\right] &\approx \left[J^{d(r)}\right]\left[\varepsilon_{dd}^{(r)}\right]\left[J^{d(r)}\right]^{\mathrm{T}} \\
\left[\varepsilon_{y\phi}^{d(r)}\right] &\approx \left[J^{d(r)}\right]\left[\varepsilon_{dd}^{(r)}\right]
\end{aligned}
\tag{15}
$$

In Equation (15), $\left[J^d\right]$ is an $N_\phi \times N_d$ matrix and is evaluated by using the adjoint method (Sykes *et al.* 1985; Liggett & Chen 1994) and the superscript T stands for the transpose. For $r \geq 1$, the covariances are evaluated according to:

$$
\varepsilon_{dd}^{(r+1)}(x_0, x_k) = \varepsilon_{dd}^{(r)}(x_0, x_k) - \sum_{i=1}^{N_\phi}\omega_{i0}^{d(r)}\varepsilon_{d\phi}^{(r)}(x_i, x_k)
\tag{16}
$$

The accuracies of the estimates at each iteration are calculated by evaluating their conditional variances $\varepsilon_{dd}(x_0, x_0)$. The smaller the variances, the more accurate the estimates. If the value of the estimate at a location is known exactly, the conditional variance at that location is zero.

After obtaining the value of $Y_d(x_0)$, the governing equations are solved again with the new value of $Y_d(x_0)$ leading to new head data $\{h\}$; then, appropriate norms of the parameters and of the heads are evaluated. If the norms are smaller than the prescribed tolerances, the iteration stops. If not, new $\left[\varepsilon_{\phi\phi}\right]$ and $\left[\varepsilon_{y\phi}\right]$ values are obtained by Equation (15), and Equation (9) is solved again with the new weights given by Equation (11) and the new head data.

NUMERICAL CASE STUDY

To test the SLE algorithm to detect the diameter distribution of an extended partial blockage, the geometry of the pipe system in Figure 2(b) was used. A reservoir was present at node R with a hydraulic constant head of 80 m, while at node V, there was a partially open valve discharging 0.04 m^3/s into the atmosphere under steady-state conditions.

The pipe was $L = 2,000$ m long, with a diameter equal to $D_i = 0.2$ m. The roughness of the pipe was 3.5 mm. For the transient simulation, the friction head losses were evaluated by means of the Darcy–Weisbach formula considering the flow as completely turbulent; the pressure wave speed was assumed equal to 1,000 m/s.

The diameter distribution resulting from the formation of the blockage was simulated by 500 random diameters (the pipe was divided into 500 blocks, of length 4 m each), and was obtained by assigning a random reduction $r(x)$ to each block by means of a stochastic random field generator (Gutjahr 1989). Eventually, the diameters were obtained by $D(x) = D_i - r(x)$. The mean and the variance of the reduction $r(x)$ were set to $m_r = 0.03$ m and $\sigma_r = 0.0006$ m^2, respectively; the spatial correlation scale of $r(x)$ was $\gamma = 160$ m.

For the estimation, the following information was used:

1. Twenty diameter measurements along the pipe (primary information), shown in Table 1 and Figure 3.
2. Transient head data acquired for 5 s at a rate of 250 Hz at valve V (hereinafter referred to as the pressure signal) used as secondary information (Figure 4). The pressure signal was obtained by means of a fast closure maneuver of the valve V, which was simulated by Equation (6). The procedure to properly execute fast maneuvers and to generate sharp pressure waves is widely discussed in Brunone *et al.* (2008b) and Meniconi *et al.* (2011b).

In the following, the results of the estimation obtained by means of the SLE are compared with those achieved by kriging and co-kriging. Kriging used only measured diameters, co-kriging linearly included the pressure signal as well as the measured diameters, while, as discussed above, the SLE considered the measured diameters and the successive inclusion of the pressure signal.

Table 1 | Measured diameter along the pipe

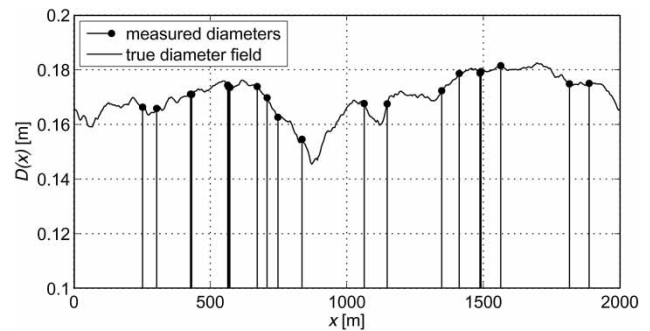| x [m]	Measured diameter [m]
251	0.179
304	0.170
428	0.179
432	0.170
565	0.167
567	0.172
572	0.182
672	0.166
708	0.175
747	0.174
836	0.166
1,064	0.174
1,147	0.175
1,348	0.174
1,411	0.171
1,489	0.155
1,492	0.166
1,563	0.179
1,816	0.163
1,887	0.174

Figure 3 | True and measured diameters at the observation locations.

By taking advantage of the primary information (i.e. the 20 diameter measurements) a variogram analysis was carried out, giving the experimental variogram in Figure 5. It was then fitted with an exponential model obtaining a range of 480 m, a sill of 0.003 m^2 and a nugget of 5.13×10^{-5} m^2.

Because of the available computational resources, in the estimation procedure, the pipe was parametrized into $N_{D\text{est}}$ blocks. After some simulations $N_{D\text{est}}$ was chosen equal to
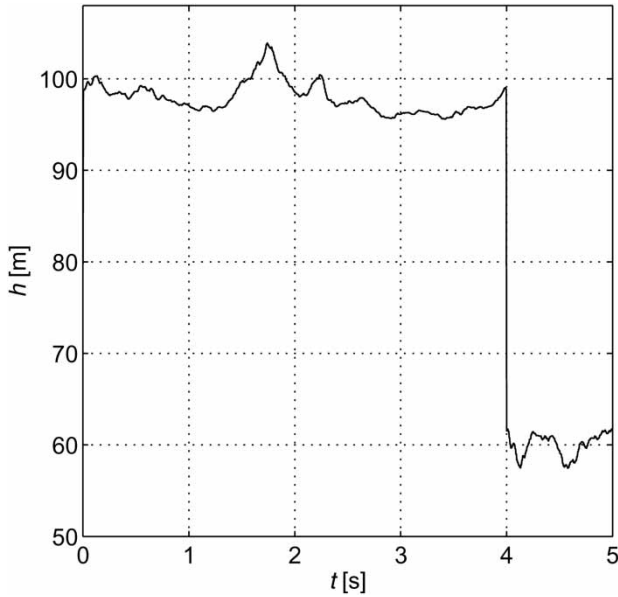
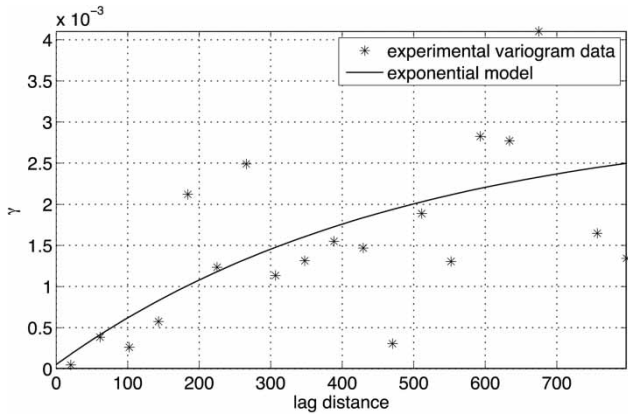**Figure 4** │ Pressure signal available at valve *V*.

Figure 5 │ Variogram analysis on the measured diameters. Experimental variogram and its fitted exponential model.

100, allowing a reasonable compromise between the description of the diameter variability and the computational times. The parametrization led to a spatial resolution $\Delta_x = 20$ m. Since Δ_x is directly related to the time step Δ_t of the forward simulation through the Courant conditions $\frac{c\Delta_t}{\Delta_x} \leq 1$; $N_h = 252$ head values were extracted from the pressure signal in Figure 4.

The SLE converged in five iterations with a computational time of 1,469 s (CPU Intel Core Duo 2.16 Ghz, RAM 4 Gb). To stop the iterative procedure, one of the following criteria had to be satisfied.

1. The mean squared differences between true and modeled heads:

$$L_{2h} = \frac{1}{N_h}\sqrt{\sum_{i=1}^{N_h}(h_{est}^i - h_{true}^i)^2} \leq 10^{-3}\,\text{m} \tag{17}$$

2. The change between two successive iterations of the average absolute error of the diameters:

$$L_{1d} = \frac{1}{N_{D_{est}}}\sum_{i=1}^{N_{D_{est}}}\left|D_i^{r+1} - D_i^{r+1}\right| \leq 10^{-5}\,\text{m} \tag{18}$$

3. The number of iterations is less than 40.

Figure 6 compares the true and the estimated diameters along the location x of the pipe obtained for kriging, co-kriging and SLE techniques. It can be clearly seen that the best estimate is obtained by means of the SLE. Note that co-kriging improves the estimation close to $x = 0$ m with respect to the kriging case due to the inclusion of the pressure signal at valve V. In Figure 7, the relative percentage errors $\Delta_d = \frac{D_{true} - D_{est}}{D_{true}}100$ obtained for kriging, co-kriging and the SLE are plotted (D_{true} = true diameter, D_{est} = estimated diameter). Again, the smallest values of the relative errors are provided by the SLE ($|\Delta_d| \leq 2\%$).

Table 2 shows a statistical analysis of the relative errors of Figure 7. The mean and the variance of Δ_d for the SLE are
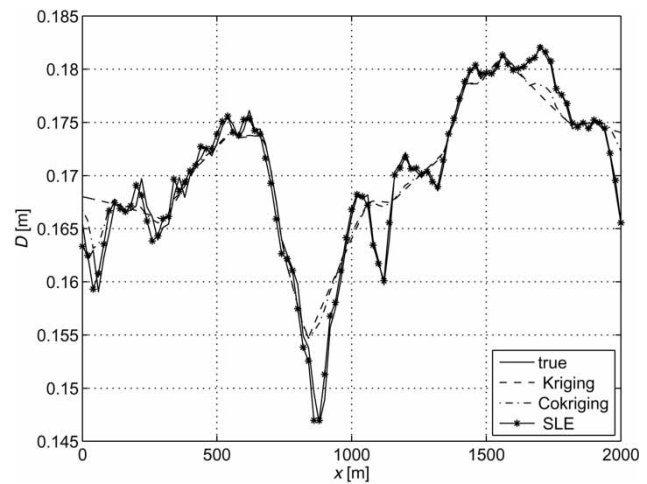

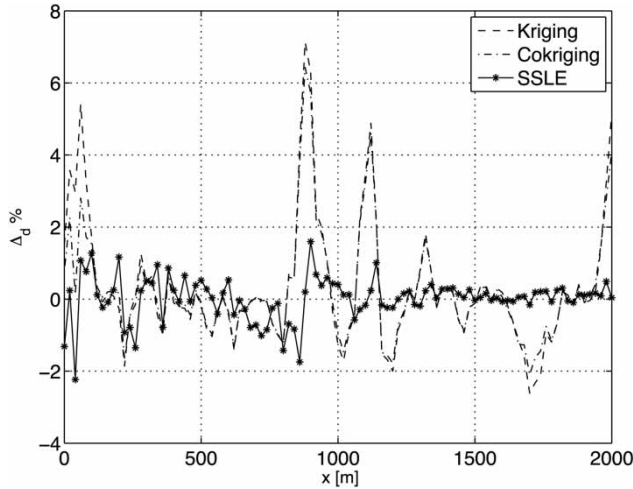**Figure 6** │ Estimated and true diameters along *x* for kriging, co-kriging and the SLE.

Figure 7 | Relative errors between estimated and true diameters along *x* of the pipe for kriging, co-kriging and the SLE.

Table 2 | Statistical analysis of relative percentage errors obtained in the estimation for kriging, co-kriging and the SLE

Technique	Mean of Δ_d [%]	Variance of Δ_d	Max of Δ_d [%]	MSE [m]
Kriging	0.35	3.20	7.13	0.181×10^{-2}
Co-kriging	0.27	2.24	6.42	0.151×10^{-2}
SLE	0.014	0.35	2.23	0.591×10^{-3}

about an order of magnitude smaller with respect to the kriging and co-kriging. Also, in terms of the mean squared error (MSE), the SLE behaves much better than the other two techniques providing a value of 0.591×10^{-3} m with respect to 0.181×10^{-2} m and 0.151×10^{-2} m for kriging and co-kriging, respectively.

Figure 8 compares the scatter plots between true and estimated diameters obtained by the co-kriging and the SLE, respectively. While estimated diameters for the SLE are very close to the $45°$ line, for kriging and co-kriging, they spread out around it. To quantify the agreement between the true and estimated diameters, a linear fitting of the data in Figure 8 has been carried out for the three techniques. The results are shown in Table 2. The goodness of fit is measured using the correlation coefficient:

$$\rho = \frac{\text{Cov}(D_{\text{true}}, D_{\text{est}})}{\sqrt{\text{Var}(D_{\text{true}})\text{Var}(D_{\text{est}})}} \tag{19}$$

and D_{y0} and *s*. These latter two parameters describe the fitting line function. For such a line, the closer the slope coefficient and the *y*-intercept are to 1 and 0, respectively, the better the diameters are estimated. Table 3 clearly confirms the good results obtained with the use the SLE with respect to the two classic geostatistic techniques.

Figure 9 plots the frequency distribution of the difference between the true log-diameters and those estimated along with their normal distribution (mean $\mu = 1.21 \times 10^{-4}$ m, standard deviation $\sigma = \pm 0.0060$ m). To verify if the log-errors follow the normal distribution, a Kolmogorov–Smirnov test was performed (Massey 1951). The null hypothesis is that the error has a standard normal distribution. The test rejects the null hypothesis at 5%significance, suggesting the unbiasedness of the estimator.

Figure 10 plots the conditional variance of the estimated diameters for kriging, co-kriging and the SLE. The inclusion of heads measured at location *V* by co-kriging reduces the uncertainty (conditional variance of estimated diameters) with respect to the kriging. In particular, the accuracy increases close to the measurement section *V*, while it stays low close to the diameter measurement locations. On average, the inclusion of the head data improves the accuracy. When the heads are included successively via the SLE, the variance decreases to about 10^{-10} m^2 (it lies on the *x*-axis of Figure 10), which is a lower order of magnitude with respect to the kriging and co-kriging techniques, confirming the results obtained with the analysis of the relative errors.

CONCLUSIONS

In this paper, a stochastic linear estimator, previously used in groundwater inverse problems by Yeh *et al.* (1996), has been applied to detect size and position of the extended partial blockages by estimating their diameter distribution. With such an estimator, the diagnosis of pipe systems is cast in the probabilistic framework by treating the parameters as a stochastic process. The SLE allows embedding of the primary information of the parameters in the estimation procedure and the use of transient pressure signals to improve the accuracy of the estimates. The availability of the primary information is not a limitation since the SLE can even use head measurements only to estimate the diameter
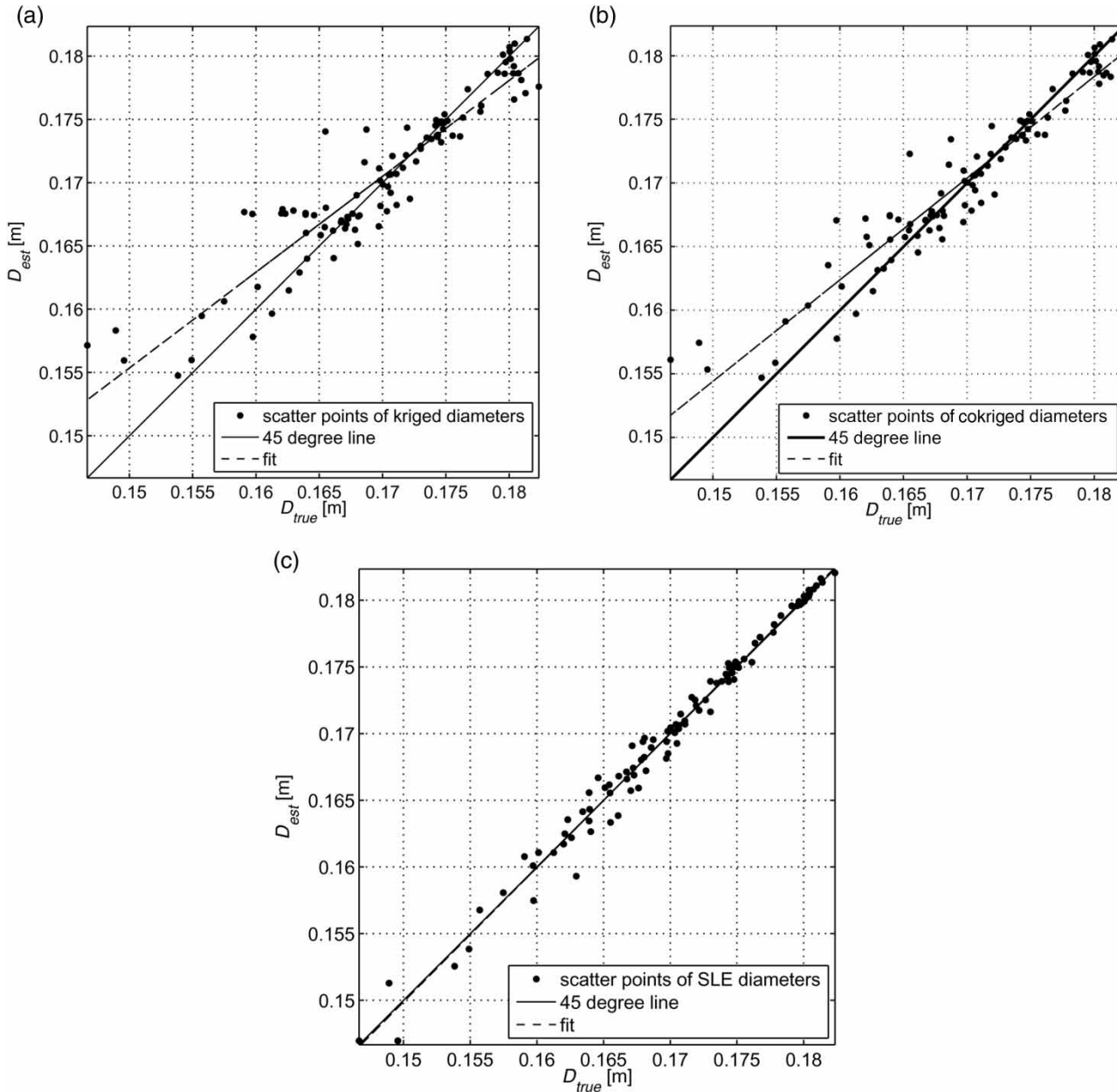
Figure 8 | Scatter plots between true and estimated diameters for (a) kriging, (b) co-kriging and (c) the SLE.

Table 3 | Results of the linear fitting between true and estimated diameters for kriging, co-kriging and the SLE

Technique	y-intercept D_{y0} [m]	Slope coefficient s	Correlation coefficient ρ
Kriging	0.0418	0.7573	0.9357
Co-kriging	0.0345	0.7990	0.9581
SLE	−0.0011	1.0069	0.9922

distribution of the pipe. The algorithm is able to assess the uncertainty associated with the estimates by the evaluation of the conditional variance of the parameters.

In the numerical example presented in this paper, it is shown that the SLE performs much better than classical geostatistical techniques such as kriging and co-kriging, allowing the non-linearity associated with the information provided by the transient tests to be taken into account. For these reasons,
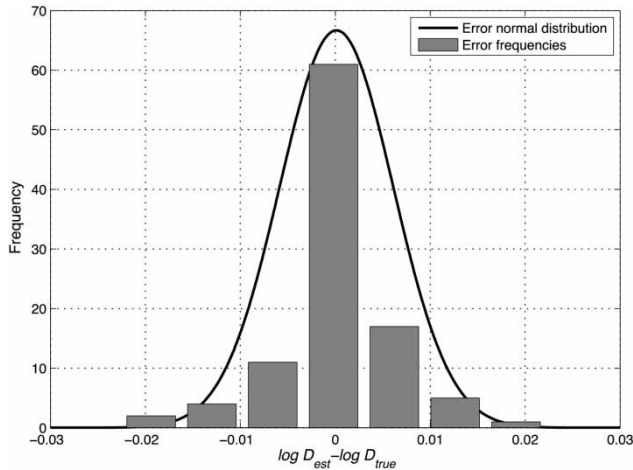
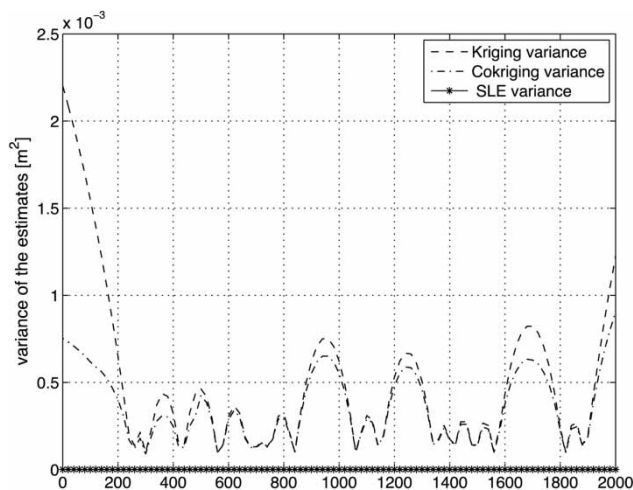**Figure 9** | Frequency of the log-error of the diameters and their normal distribution.

Figure 10 | Variance of the estimated diameters along location x of the pipe for kriging, co-kriging and the SLE.

the SLE appears to be a promising technique that can be applied to pipe system diagnosis. Indeed, further studies and extensive experimental testing are required to assess the reliability and the potential of this technique.

ACKNOWLEDGEMENTS

REFERENCES

Brunone, B. 1999 Transient test-based technique for leak detection in outfall pipes. *Journal of Water Resources Planning and Management* **125** (5), 302–306.

Brunone, B. & Ferrante, M. 2001 Detecting leaks in pressurised pipes by means of transients. *Journal of Hydraulic Research* **39** (5), 539–547.

Brunone, B., Ferrante, M. & Meniconi, S. 2008a Discussion of 'Detection of partial blockage in single pipelines' by P. K. Mohapatra, M. H. Chaudhry, A. A. Kassem & J. Moloo *Journal of Hydraulic Engineering* **134** (6), 872–874.

Brunone, B., Ferrante, M. & Meniconi, S. 2008b Portable pressure wave-maker for leak detection and pipe system characterization. *Journal of American Water Works Association* **100** (4), 108–116.

Dettinger, M. D. & Wilson, J. L. 1981 First order analysis of uncertainty in numerical models of groundwater flow part: 1. Mathematical development. *Water Resources Research* **17** (1), 149–161.

Duan, H. F., Lee, J. P., Ghidaoui, S. M. & Tung, Y.-K. 2012 Extended blockage detection in pipelines by using the system frequency response analysis. *Journal of Water Resources Planning and Management* **138** (1), 55–62.

Ferrante, M. & Brunone, B. 2003a Pipe system diagnosis and leak detection by unsteady-state tests. 1. Harmonic analysis. *Advances in Water Resources* **26** (1), 95–105.

Ferrante, M. & Brunone, B. 2003b Pipe system diagnosis and leak detection by unsteady-state tests. 2. Wavelet analysis. *Advances in Water Resources* **26** (1), 107–116.

Ferrante, M., Brunone, B. & Meniconi, S. 2009 Leak detection in branched pipe systems coupling wavelet analysis and a Lagrangian model. *Journal of Water Supply: Research and Technology* **58** (2), 95–106.

Fletcher, J. 1988 *Computational Techniques for Fluid Dynamics*, vol. 1. Springer Verlag, New York.

Gooch, R. M., Clarke, T. A. & Ellis, T. J. 1996 A semi-autonomous sewer surveillance and inspection vehicle. In: *Intelligent Vehicles Symposium, Proceedings of IEEE*, Seikei University, Tokyo, Japan, 1996, pp. 64–69.

Gutjahr, A. L. 1989 Fast Fourier Transforms for Random Field Generation. Project Report for Los Alamos Grant to New Mexico Tech, New Mexico Institute of Mining and Technology, Socorro.

Haghighi, A. & Keramat, A. 2012 A fuzzy approach for considering uncertainty in transient analysis of pipe networks. *Journal of Hydroinformatics* **14** (4), 1024.

Hoeksema, R. J. & Kitanidis, P. K. 1984 An application of the geostatistical approach to the inverse problem in two-dimensional groundwater modeling. *Water Resources Research* **20** (7), 1003–1020.

Hunt, A. 1996 Fluid properties determine flow line blockage potential. *Oil & Gas Journal* **94** (29), 62–66.

Illman, W. A. & Liu, X. 2007 Steady-state hydraulic tomography in a laboratory aquifer with deterministic heterogeneity: multi-method and multiscale validation of hydraulic conductivity tomograms. *Journal of Hydrology* **341** (3–4), 222–234.

Illman, W. A., Zhu, J., Craig, A. J. & Yin, D. 2010 Comparison of aquifer characterization approaches through steady state groundwater model validation: a controlled laboratory sandbox study. *Water Resources Research* **46**, W04502.

Kapelan, Z. S., Savic, D. A. & Walters, G.-A. 2003 A hybrid inverse transient model for leakage detection and roughness calibration in pipe networks. *Journal of Hydraulic Research* **41** (5), 481–492.

Kitanidis, P. K. & Vomvoris, E. G. 1983 A geostatistical approach to the inverse problem in groundwater modeling (steady state) and one-dimensional simulations. *Water Resources Research* **19** (3), 677–690.

Lee, P. J., Vitkovsky, J. P., Lambert, M. F., Simpson, A. R. & Liggett, J. A. 2008 Discrete blockage detection in pipelines using the frequency response diagram: numerical study. *Journal of Hydraulic Engineering* **134** (5), 658–663.

Liggett, J.-A. & Chen, L. C. 1994 Inverse transient analysis in pipe networks. *Journal of Hydraulic Engineering* **120** (8), 934–955.

Massari, C., Yeh, T.-C. J., Ferrante, M., Brunone, B. & Meniconi, S. 2012 Detection of partial extended blockages by means of a stochastic successive linear estimator. In: *10th International Conference on Hydroinformatics* (R. Hinkelmann, M. H. Nasermoaddeli, S. Y. Liong, D. Savic, P. Fröhle & K. F. Daemrich, eds), 14–18 July 2012, Hamburg.

Massey, F. J. 1951 The Kolmogorov-Smirnov test for goodness of fit. *Journal of the American Statistical Association* **46** (253), 68–78.

Meniconi, S., Brunone, B., Ferrante, M. & Massari, C. 2011a Fast transients as a tool for partial blockage detection in pipes: first experimental results. In: *12th Annual Water Distribution Systems Analysis Conference, WDSA 2010* (K. Lansey, C. Choi, A. Ostfeld & I. Pepper, eds), September 2010, Tucson, AZ, pp. 144–153.

Meniconi, S., Brunone, B., Ferrante, M. & Massari, C. 2011b Small amplitude sharp pressure waves to diagnose pipe systems. *Water Resources Management* **25** (1), 79–96.

Meniconi, S., Brunone, B., Ferrante, M. & Massari, C. 2011c Transient tests for locating and sizing illegal branches in pipe systems. *Journal of Hydroinformatics* **13** (3), 334–345.

Meniconi, S., Brunone, B. & Ferrante, M. 2011d In-line pipe device checking by short period analysis of transient tests. *Journal of Hydraulic Engineering* **137** (7), 713–722.

Meniconi, S., Brunone, B. & Ferrante, M. 2012 Water-hammer pressure waves interaction at cross-section changes in series in viscoelastic pipes. *Journal of Fluids and Structures* **33** (2012), 44–58.

Mohapatra, P. K., Chaudhry, M. H., Kassem, A. A. & Moloo, J. 2006 Detection of partial blockage in single pipelines. *Journal of Hydraulic Engineering* **132** (2), 200–206.

Pasha, M. F. K. & Lansey, K. 2010 Effect of parameter uncertainty on water quality predictions in distribution systems-case study. *Journal of Hydroinformatics* **12** (1), 1.

Scott, S. L. & Satterwhite, L. A. 1998 Evaluation of the backpressure technique for blockage detection in gas flowlines. *Journal of Energy Resources Technology* **120** (1), 27–31.

Scott, S. L. & Yi, J. 1999 Flow testing methods to detect and characterize partial blockages in looped subsea flowlines. *Journal of Energy Resources Technology* **121** (3), 154–160.

Sharma, A., Sandhu, B. S. & Singh, B. 2010 Incoherent scattering of gamma photons for non-destructive Tomographic Inspection of Pipeline. *Applied Radiation and Isotopes Including Data Instrumentation and Methods for Use in Agriculture Industry and Medicine* **68** (12), 2181–2188.

Sun, S., Khu, S. T., Kapelan, Z. & Djordjević, S. 2011 A fast approach for multiobjective design of water distribution networks under demand uncertainty. *Journal of Hydroinformatics* **13** (2), 143.

Sykes, J. F., Wilson, J. L. & Andrews, R. W. 1985 Sensitivity analysis for steady state groundwater flow using adjoint operators. *Water Resources Research* **21** (3), 359–371.

Vargas-Guzmán, J. A. & Yeh, T. C. J. 2002 The successive linear estimator: a revisit. *Advances in Water Resources* **25** (7), 773–781.

Vítkovský, J., Simpson, A. & Lambert, M. 2000 Leak detection and calibration using transients and genetic algorithms. *Journal of Water Resources Planning and Management* **126** (4), 262–265.

Wang, X.-J., Lambert, M. & Simpson, A. 2005 Detection and location of a partial blockage in a pipeline using damping of fluid transients. *Journal of Water Resources Planning and Management* **131** (3), 244–249.

Wylie, E. & Streeter, V. 1993 *Fluid Transients in Systems*. Prentice-Hall, Englewood Cliffs, NJ.

Yeh, T. C. J. & Zhang, J. 1996 A geostatistical inverse method for variably saturated flow in the vadose zone. *Water Resources Research* **32** (9), 2757–2766.

Yeh, T.-C. J. & Liu, S. 2000 Hydraulic tomography: development of a new aquifer test method. *Water Resources Research* **36** (8), 2095–2106.

Yeh, T., Jin, M. & Hanna, S. 1996 An iterative stochastic inverse method: conditional effective transmissivity and hydraulic head fields. *Water Resources Research* **32** (1), 85–92.

Zhang, J. & Yeh, T. C. J. 1997 An iterative geostatistical inverse method for steady flow in the vadose zone. *Water Resources Research* **33** (1), 63–71.

Zhu, J. & Yeh, T. C. J. 2005 Characterization of aquifer heterogeneity using transient hydraulic tomography. *Water Resources Research* **41** (7), W07028.